

UC Berkeley

Basic Science

Title

Toward ZnO Light Emitting Diode

Permalink

<https://escholarship.org/uc/item/74r8z09z>

Author

Liu, Jianlin

Publication Date

2008-07-01



Fundamental Science of Energy 009

"Toward ZnO Light Emitting Diode"

Jianlin Liu

July 2008

This paper is part of the University of California Energy Institute's (UCEI) Fundamental Science of Energy Working Paper Series. UCEI is a multi-campus research unit of the University of California located on the Berkeley campus.

UC Energy Institute
2547 Channing Way, # 5180
Berkeley, California 94720-5180
www.ucei.berkeley.edu

This report was issued in order to disseminate results of and information about energy research at the University of California campuses. Any conclusions or opinions expressed are those of the authors and not necessarily those of the Regents of the University of California, the University of California Energy Institute or the sponsors of the research. Readers with further interest in or questions about the subject matter of the report are encouraged to contact the authors directly.



Proposal Title: “Toward ZnO Light Emitting Diode”

Sponsor:

UC Energy Institute

Principal Investigator:

Jianlin Liu

Department of Electrical Engineering
University of California at Riverside, Riverside, CA92521

Email: jianlin@ee.ucr.edu

Tel: (951)827-7131

Fax: (951)787-2425

1. Technical report

The project scope focuses on developing reliable p-type ZnO semiconductor materials by using plasma-assisted MBE and demonstrating feasibility of using ZnO-based materials for solid-state lighting, including fabrication, test and evaluation of proof-of-concept ZnO homo-junction LED devices. Over the two-year period July 1, 2006-June 30, 2008), we have worked on this project extensively and achieved the following research results:

1. Low-resistivity Au/Ni Ohmic contacts to Sb-doped *p*-type ZnO

ZnO is a wide band gap semiconductor material that has drawn a lot of attention recently. However, *p*-type doping is extremely difficult due to the presence of native defects and donors [U. Ozgur, Ya. I. Alivov, C. Liu, A. Teke, M. A. Reshchikov, S. Dogan, V. Avrutin, S. J. Cho, and H. Morkoc, *J Appl Phys* **98**, 041301 (2005). S. J. Pearton, D. P. Norton, K. Ip, and Y. W. Heo, *J. Vac. Sci. Technol. B* **22**, 932 (2004). D. C. Look, *Mater. Sci. Eng. B* **80**, 383 (2001)]. Active research is currently carried out to explore various suitable *p*-type dopants for ZnO [A. Tsukazaki, A. Ohtomo, T. Onuma, M. Ohtani, T. Makino, M. Sumiya, K. Ohtani, S. F. Chichibu, S. Fuke, Y. Segawa, H. Ohno, H. Koinuma, and M. Kawasaki, *Nat. Mater.* **4**, 42 (2005). D. K. Hwang, H. S. Kim, J. H. Lim, J. Y. Oh, J. H. Yang, S. J. Park, K. K. Kim, D. C. Look, and Y. S. Park, *Appl. Phys. Lett.* **86**, 151917 (2005). Y. R. Ryu, T. S. Lee, and H. W. White, *Appl. Phys. Lett.* **83**, 87 (2003). F. X. Xiu, Z. Yang, L. J. Mandalapu, J. L. Liu, and W. P. Beyermann, *Appl. Phys. Lett.* **88**, 052106 (2006). F. X. Xiu, Z. Yang, L. J. Mandalapu, and J. L. Liu, *Appl. Phys. Lett.* **88**, 152116 (2006). F. X. Xiu, Z. Yang, L. J. Mandalapu, D. T. Zhao, J. L. Liu, and W. P. Beyermann, *Appl. Phys. Lett.* **87**, 152101 (2005)]. Recently, Sb-doped ZnO films grown on Si (100) substrates exhibited reliable and reproducible *p*-type

behavior [F. X. Xiu, Z. Yang, L. J. Mandalapu, J. L. Liu, and W. P. Beyermann, Appl. Phys. Lett. **88**, 052106 (2006). F. X. Xiu, Z. Yang, L. J. Mandalapu, and J. L. Liu, Appl. Phys. Lett. **88**, 152116 (2006). F. X. Xiu, Z. Yang, L. J. Mandalapu, D. T. Zhao, J. L. Liu, and W. P. Beyermann, Appl. Phys. Lett. **87**, 152101 (2005). F. X. Xiu, Z. Yang, L. J. Mandalapu, D. T. Zhao, and J. L. Liu, Appl. Phys. Lett. **87**, 252102 (2005).]. ZnO hetero- and homo-junction devices were fabricated based on Sb-doped *p*-type ZnO films [L. J. Mandalapu, F. X. Xiu, Z. Yang, and J. L. Liu, Appl. Phys. Lett. **88**, 112108 (2006). L. J. Mandalapu, Z. Yang, F. X. Xiu, and J. L. Liu, Appl. Phys. Lett. **88**, 092103 (2006).], where Al/Ti metal was used for achieving Ohmic contacts to both *n*-type and *p*-type ZnO. However, relatively high contact resistance was observed for Al/Ti contacts on *p*-type ZnO, which limited our device performance. There are several reports on various metal schemes that have been employed for *p*-type ZnO films [J. H. Lim, K. K. Kim, D. K. Hwang, H. S. Kim, J. Y. Oh, and S. J. Park, J. of Electrochem. Soc. **152**, G179 (2005) S. Kim, B. S. Kang, F. Ren, Y. W. Heo, K. Ip, D. P. Norton, and S. J. Pearton, Appl. Phys. Lett. **84**, 1904 (2004). H. S. Yang, Y. Li, D. P. Norton, K. Ip, S. J. Pearton, S. Jang, and F. Ren, Appl. Phys. Lett. **86**, 192103 (2005). K. Ip, G. T. Thaler, H. Yang, S. Y. Han, Y. Li, D. P. Norton, S. J. Pearton, S. Jang, and F. Ren, J. Cryst. Growth **287**, 149 (2006). S. H. Kang, D. K. Hwang, and S. J. Park, Appl. Phys. Lett. **86**, 211902 (2005)]. In this letter, we explore Au/Ni metal for making Ohmic contacts to Sb-doped *p*-type ZnO films.

Sb-doped ZnO films were grown on *n*-Si(100) substrates at 550 °C using a Perkin-Elmer MBE system. Prior to growth, the Si substrates were cleaned by the Piranha-HF method and dried by nitrogen, which was followed by thermal cleaning at 650 °C. A thin undoped ZnO buffer layer was grown to improve the crystalline quality of

the subsequent Sb-doped ZnO layer. Undoped layer was grown for 30 mins while the growth of Sb-doped layer was for 150 mins, giving rise to an effective thickness of about 435 nm. Sb-doped ZnO layer was grown using Zn and Sb effusion cells. Oxygen plasma was generated by an electron-cyclotron-resonance (ECR) source. A post-growth annealing at 800 °C was carried out for 30 minutes to activate the acceptor dopants. Au/Ni bilayer metal of thickness 120/20 nm was deposited at room temperature. Rapid thermal annealing was performed at various temperatures of 700, 750, and 800 °C for 60 seconds in nitrogen environment to form Ohmic contacts. Room temperature Hall effect and resistivity measurements yielded a hole concentration, mobility, and resistivity of $1 \times 10^{19} \text{ cm}^{-3}$, $8 \text{ cm}^2\text{V}^{-1}\text{S}^{-1}$, and $0.3 \text{ } \Omega \text{ cm}$, respectively for the Sb-doped ZnO sample.

Transmission line patterns of size $75 \times 50 \text{ } \mu\text{m}$ with spacings 10, 20, 30, and $40 \text{ } \mu\text{m}$ were fabricated by *e*-beam evaporation and lift off. The fabricated patterns are shown as the inset of Fig.1.

Current-voltage (*I-V*) characteristics of these contacts were measured using 4155C parameter analyzer and

Signatone probe station. The point of probing is shown by the arrows on a pair of contacts of the TLM pattern. As-deposited contacts were found to be rectifying with very

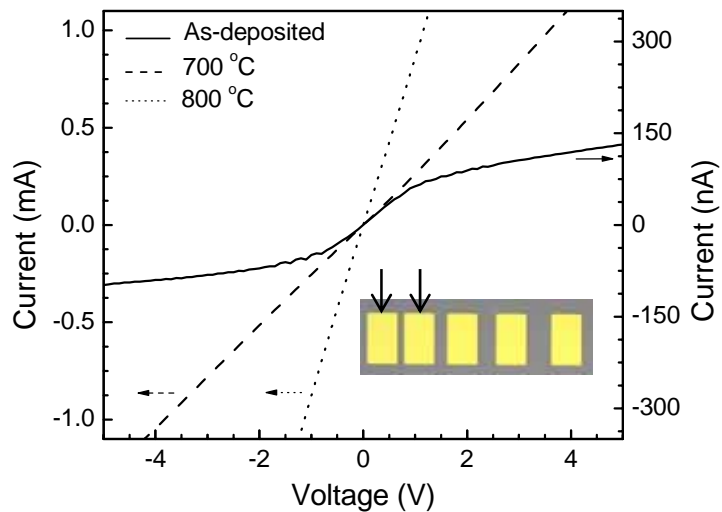


Figure 1 *I-V* characteristics of as-deposited contacts (solid line), annealed contacts at 700 °C (dashed line), and 800 °C (dotted line). The arrows show the point of probing on the schematic of the TLM patterns in the inset.

high contact resistance as shown by the solid I - V curve in Fig. 1. The current conducted through them is of the order of nA. Figure 1 also shows the linear I - V characteristics indicating the establishment of Ohmic conduction for contacts that are annealed at 700 °C (dashed) and 800 °C (dotted). The contact resistance was found to decrease with the increase of annealing temperature, as seen from the increase in magnitude of current. The total resistance, which includes contact

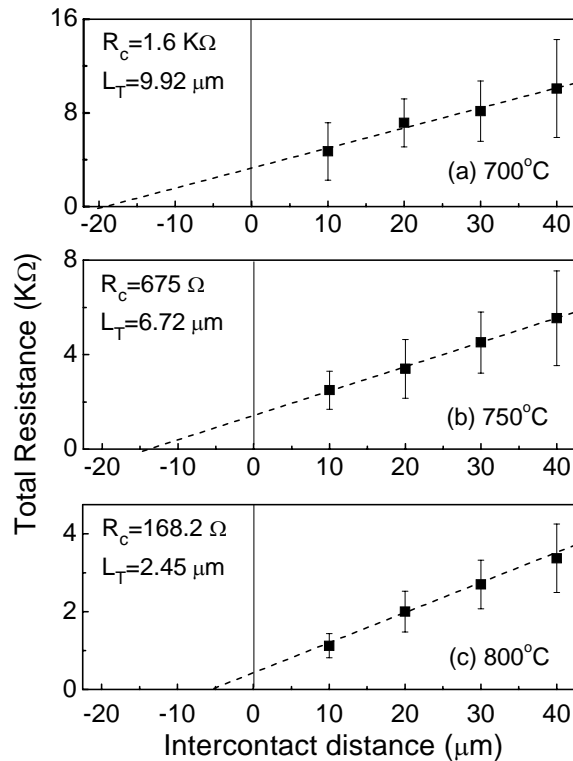


Figure 2 Contact resistance as a function of intercontact distance for the samples annealed at (a) 700, (b) 750, and (c) 800 °C, respectively. The linear characteristics are extrapolated to obtain specific contact resistivity.

resistivity of about $3.0 \times 10^{-4} \Omega \text{ cm}^2$ was then calculated.

The annealing temperature dependence of specific contact resistivity of samples is shown in Fig. 3. Although Ohmic contacts were established at 700 °C, the specific

resistance, was calculated from the slopes of I - V curves. A number of TLM patterns were measured and the total resistance with error factor was plotted as a function of the inter-contact distance for all the annealed samples. Figures 2(a)-(c) show TLM result of the samples which were annealed at 700, 750, and 800 °C for 60 s. The linear characteristic was extrapolated to obtain the contact resistance and transfer length. For example, for the sample annealed at 800 °C, these values are of 168.2 Ω and 2.45 μm , respectively. The specific contact

contact resistivity of the sample was relatively high at about $1.2 \times 10^{-2} \Omega \text{ cm}^2$. The specific contact resistivity decreases noticeably with increasing annealing temperature. The lowest value of $3.0 \times 10^{-4} \Omega \text{ cm}^2$ is obtained for the sample annealed at 800 °C, which is about two orders of magnitude lower than that for 700 °C. As a matter of fact, the values are comparable with the contact resistivities of the Ohmic contacts to phosphorus-doped *p*-type ZnO which are low enough for exploring efficient optoelectronic devices [J. H. Lim, K. K. Kim, D. K. Hwang, H. S. Kim, J. Y. Oh, and S. J. Park, *J. of Electrochem. Soc.* **152**, G179 (2005) S. Kim, B. S. Kang, F. Ren, Y. W. Heo, K. Ip, D. P. Norton, and S. J. Pearton, *Appl. Phys. Lett.* **84**, 1904 (2004). H. S. Yang, Y. Li, D. P. Norton, K. Ip, S. J. Pearton, S. Jang, and F. Ren, *Appl. Phys. Lett.* **86**, 192103 (2005)].

To understand possible reason of Ohmic contact formation on Sb-doped *p*-type films, secondary ion mass spectroscopy (SIMS) measurements were carried out to obtain the Zn, O, Au, Ni, and Si elemental profiles of the samples before and after annealing.

ZnO layer on Si substrate, thin layer of Ni, and thick layer of Au are clearly identified in Fig.4 (a) for the as-deposited sample. The profiles are distinct without noticeable inter-diffusion between metal and ZnO. For the sample annealed at 700 °C as shown in Fig. 4

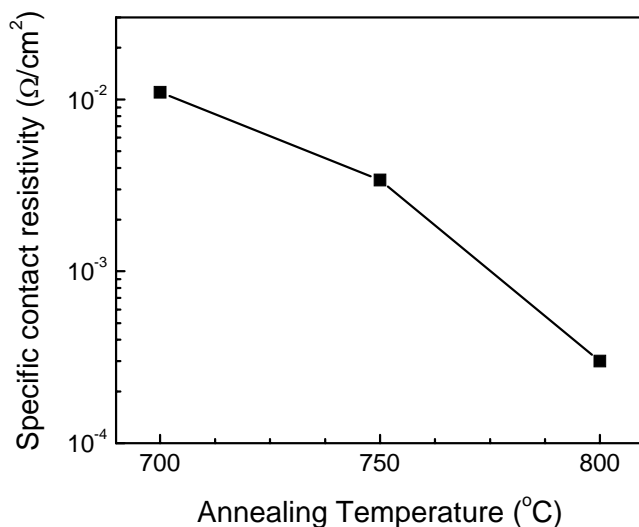


Figure 3 Specific contact resistivity as a function of annealing temperature on a semilog plot. The lowest resistivity of $3.0 \times 10^{-4} \Omega \text{ cm}^2$ is obtained for the sample annealed at 800 °C.

(b), inter-diffusion of Zn, O with Ni and Au can be observed. O at the surface has increased while Au has decreased slightly. This is due to the surface oxidation during thermal annealing. Out-diffusion of Zn is also observed, which may be responsible for the formation of Ohmic contacts. Out-diffusion of Zn creates Zn vacancies in the ZnO film [H. S. Yang, Y. Li, D. P. Norton, K. Ip, S. J. Pearton, S. Jang, and F. Ren, Appl. Phys. Lett. **86**, 192103 (2005)]. Zn vacancies by themselves produce acceptor levels that

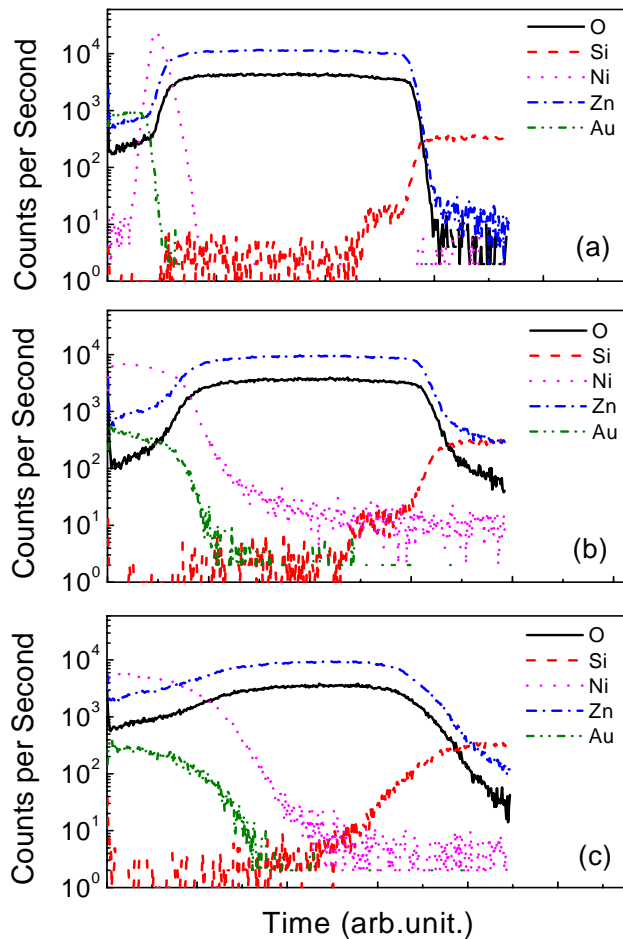


Figure 4 (Color online) Elemental profiles of Au, Ni, Zn, O, and Si from samples with contacts (a) as-deposited, (b) annealed at 700 °C, and (c) annealed at 800 °C, respectively.

are relatively deep. However, these vacancies can couple with activated Sb atoms to form $Sb_{Zn}+2V_{Zn}$ and produce shallow acceptor levels [F. X. Xiu, Z. Yang, L. J. Mandalapu, D. T. Zhao, and J. L. Liu, Appl. Phys. Lett. **87**, 252102 (2005). S. Limpijumnong, S. B. Zhang, S. H. Wei, and C. H. Park, Phys. Rev. Lett. **92**, 155504 (2004)]. This helps to form low-resistance contacts as the depletion region of the Schottky diode becomes very thin due to strong *p*-type behavior and holes can tunnel through easily. The sample

annealed at 800 °C as shown in Fig. 4 (c) confirms further out-diffusion of Zn, creating

more Zn vacancies and hence, better contact resistivity through increased hole concentration.

In summary, Au/Ni Ohmic contacts to Sb-doped *p*-type ZnO film were achieved by rapid thermal annealing. The lowest specific contact resistivity of $3.0 \times 10^{-4} \Omega \text{ cm}^2$ was obtained for the contacts annealed at 800 °C. The possible reason for the formation of Ohmic contacts involves an original high hole concentration of $1 \times 10^{19} \text{ cm}^{-3}$ and the formation of additional Zn vacancies, which couple with activated Sb atoms to increase the local hole concentration. These results suggest that Au/Ni is very good metal combination to form Ohmic contacts on Sb-doped *p*-type ZnO for optoelectronic device applications.

2. Sb-doped p-ZnO/Ga-doped n-ZnO homojunction ultraviolet light emitting diodes

ZnO has recently been extensively studied due to its wide band gap and large exciton binding energy for ultraviolet (UV)/blue optoelectronic applications such as light emitting diodes (LEDs) and laser diodes [Ü. Özgür, Ya. I. Alivov, C. Liu, A. Teke, M. A. Reshchikov, S. Dogan, V. Avrutin, S.-J. Cho, and H. Morkoç, *J. Appl. Phys.* **98**, 041301 (2005) S. J. Pearton, D. P. Norton, K. Ip, Y. W. Heo, and T. Steiner, *J. Vac. Sci. Technol. B* **22**, 932 (2004). D. C. Look, *Mater. Sci. Eng. B* **80**, 383 (2001).D. C. Look, B. Claflin, Y. I. Alivov, and S. J. Park, *Phys. Status Solidi A* **201**, 2203 (2004).]. Although it is extremely difficult to achieve reliable p-type ZnO due to compensation effect from shallow donors induced during material growth, many research groups have reported p-type ZnO and ZnO LEDs using various dopants such as N [A. Tsukazaki, A. Ohtomo, T. Onuma, M. Ohtani, T. Makino, M. Sumiya, K. Ohtani, S. F. Chichibu, S. Fuke, Y. Segawa, H. Ohno, H. Koinuma, and M. Kawasaki, *Nat. Mater.* **4**, 42 (2005). D. C. Look, D. C. Reynolds, C. W. Litton, R. L. Jones, D. B. Eason, and G. Cantwell, *Appl. Phys. Lett.* **81**, 1830 (2002). K. W. Liu, D. Z. Shen, C. X. Shan, J. Y. Zhang, B. Yao, D. X. Zhao, Y. M. Lu, and X. W. Fan, *Appl. Phys. Lett.* **91**, 201106 (2007).F. X. Xiu, Z. Yang, L. J. Mandalapu, J. L. Liu, and W. P. Beyermann, *Appl. Phys. Lett.* **88**, 052106 (2006). J. H. Lim, C. K. Kang, K. K. Kim, I. K. Park, D. K. Hwang, and S. J. Park, *Adv. Mater.* **18**, 2720 (2006). D. K. Hwang, M. S. Oh, J. H. Lim, C. G. Kang, and S. J. Park, *Appl. Phys. Lett.* **90**, 021106 (2007)], As [Y. R. Ryu, T. S. Lee, J. A. Lubguban, H. W. White, B. J. Kim, Y. S. Park, and C. J. Youn, *Appl. Phys. Lett.* **88**, 241108 (2006). J. C. Sun, J. Z. Zhao, H. W. Liang, J. M. Bian, L. Z. Hu, H. Q. Zhang, X. P. Liang, W. F. Liu, G. T. Du, *Appl. Phys. Lett.* **90**, 121128 (2007)], and other specific techniques. Previously, Sb-

doped p-type ZnO and p-n homojunction were studied by our group [F. X. Xiu, Z. Yang, L. J. Mandalapu, D. T. Zhao, and J. L. Liu, Appl. Phys. Lett. **87**, 252102 (2005). L. J. Mandalapu, F. X. Xiu, Z. Yang, and J. L. Liu, Appl. Phys. Lett. **88**, 112108 (2006). L. J. Mandalapu, Z. Yang, F. X. Xiu, and J. L. Liu, Appl. Phys. Lett. **88**, 092103 (2006).], however no UV emissions were reported. In this letter, we report homojunction LEDs based on Sb-doped p-type ZnO that show strong near band edge (NBE) emissions at low temperatures and room temperature.

ZnO homojunction was grown on n-type Si (100) substrate (1-20 Ωcm) using molecular beam epitaxy (MBE) system. First, a thin MgO buffer layer was deposited at 350 $^{\circ}\text{C}$ for 5min to reduce the lattice mismatch between Si and ZnO [M. Fujita, M. Sasajima, Y. Deesirapipat, and Y. Horikoshi, J. Cryst. Growth **278**, 293 (2005)], which was followed by the growth of a ZnO buffer layer at the same substrate temperature for 15 min. Then, the two layer structured Sb-doped p-type ZnO/Ga-doped n-type ZnO homojunction was grown on this MgO/ZnO buffer. The 420nm thick Ga-doped ZnO film was deposited at a substrate temperature of 450 $^{\circ}\text{C}$ and Zn and Ga effusion cells temperatures of 380 $^{\circ}\text{C}$ and 520 $^{\circ}\text{C}$, respectively. This was followed by the growth of the 420nm thick Sb-doped ZnO layer under oxygen rich condition with a higher substrate temperature of 550 $^{\circ}\text{C}$. During the growth of this layer, Zn and Sb effusion cell temperatures were 380 $^{\circ}\text{C}$ and 360 $^{\circ}\text{C}$, respectively. In-situ thermal activation of the Sb dopant was performed in vacuum at 750 $^{\circ}\text{C}$ for 20 min.

Homojunction LEDs were fabricated by standard photolithography techniques. Mesa size of 800 $\mu\text{m} \times 800 \mu\text{m}$ were defined. Transmission line method (TLM) patterns with the size of 75 $\mu\text{m} \times 50 \mu\text{m}$ and intercontact spacings of 10, 20, 30, 40 μm were

made simultaneously to study the contact properties. Etching was done using ammonium chloride hydroxide buffer solution to reach down to the n-type ZnO layer for n-type contacts with the etching rate of about 10 nm/min. Au/NiO and Au/Ti contacts of thicknesses of 500/30 and 150/30 nm were deposited on p-type Sb-doped ZnO and n-type Ga-doped ZnO layer by e-beam evaporation, respectively. The contacts were subjected to rapid thermal annealing in nitrogen ambience to form Ohmic contacts. The annealing conditions of Au/NiO and Au/Ti contacts were 800 °C for 120 s and 400 °C for 60 s, respectively.

Current-Voltage (I-V) characteristics were measured using Agilent 4155C semiconductor parameter analyzer. I-V curve in semi-logarithmic scale of a typical device is shown in Fig. 5. The turn-on voltage of this diode is about 6 V, and the large turn-on voltage of the diode involves the effects from the voltage drop on the contact and p-type layer. The inset (a) of Fig. 5 gives the surface intercontact I-V curves of Au/NiO contacts on p-type ZnO and Au/Ti contacts on n-type ZnO, respectively, indicating Ohmic contact behavior. The electrical properties of the n-type ZnO layer was determined by Hall effect measurement in a van der Pauw configuration after the p-type ZnO layer was etched. Electron concentration, mobility, resistivity of $2.8 \times 10^{19} \text{ cm}^{-3}$, $8.7 \text{ cm}^2\text{V}^{-1}\text{S}^{-1}$, and $0.02 \text{ } \Omega \text{ cm}$, respectively were obtained. For this multilayer structured device, electrical properties in p-type ZnO layer cannot be reliably obtained by Hall effect measurement. Nevertheless, p-type behavior of Sb-doped ZnO layer is evident from the rectifying diode characteristics. Low resistivity contacts are very important to ensure the high efficiency of ZnO optoelectronic device performance. Since we have relatively lightly doped p-type ZnO layer, Au/NiO contacts rather than Au/Ni contacts [L.

J. Mandalapu, Z. Yang, and J. L. Liu, Appl. Phys. Lett. **90**, 252103 (2007).] are chosen to form Ohmic contacts to the film in the devices. The total resistances (in TLM patterns) were plotted against the intercontact distance in the inset (b) of Fig. 5. The contact resistance and transfer length are 260.4Ω and $3.77 \mu\text{m}$, which were extrapolated from linear fitting. Then the specific contact resistivity of $7.4 \times 10^{-4} \Omega \text{cm}^2$ was calculated. This value is much smaller than that of the Au/Ni ($7.6 \times 10^{-3} \Omega \text{cm}^2$) contacts on another piece of the same p-type ZnO layer. Furthermore, Au/Ni (500nm/30nm) contacts need much higher annealing temperature to form reasonable Ohmic conduction ($960 \text{ }^\circ\text{C}$). Such a high temperature would potentially degrade the contact morphology and film quality. The advantage of Au/NiO contacts results from high p-type conductivity of NiO [H. Ohta, M. Hirano, K. Nakahara, H. Maruta, T. Tanabe, M. Kamiya, T. Kamiya, and H. Hosono, Appl. Phys. Lett. **83**, 1029 (2003).], and also the outdiffusion of oxygen could be reduced

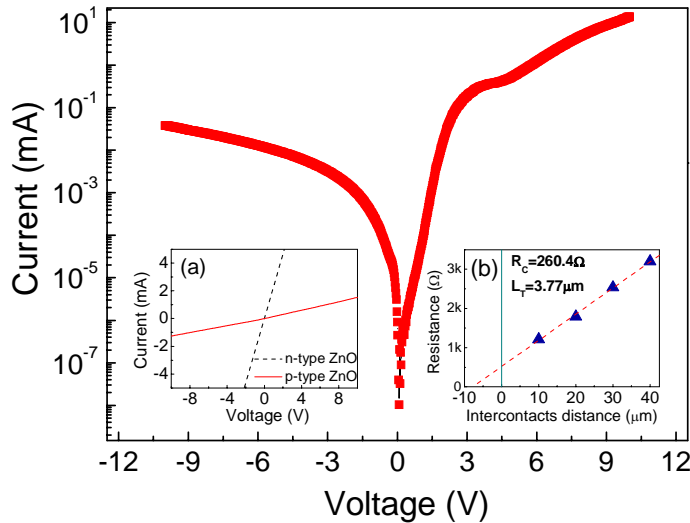


Figure 5 Semi-logarithmic scale I-V characteristics of the p-type Sb-doped ZnO/n-type Ga-doped ZnO homojunction. Inset (a) shows the surface p-p contacts and n-n contacts I-V curves, respectively. Ohmic contacts behaviors are evident. Inset (b) gives the intercontact resistance as a function of intercontact distance for Au/NiO on p-type ZnO layers. Linear fitting was used to obtain the specific contact resistivity.

to depress oxygen vacancy in the film [L. J. Mandalapu, Z. Yang, and J. L. Liu, Appl. Phys. Lett. **90**, 252103 (2007).].

Electroluminescence (EL)

characterizations were performed by using home-built measurement set-up including an Oriel monochromator and a lock-in amplifier with chopper. Temperature dependent EL spectra under 30 mA forward injection current are shown in Fig. 6. For the device operated at 9 K, the spectrum is dominated by a peak at 373.5 nm (3.32 eV).

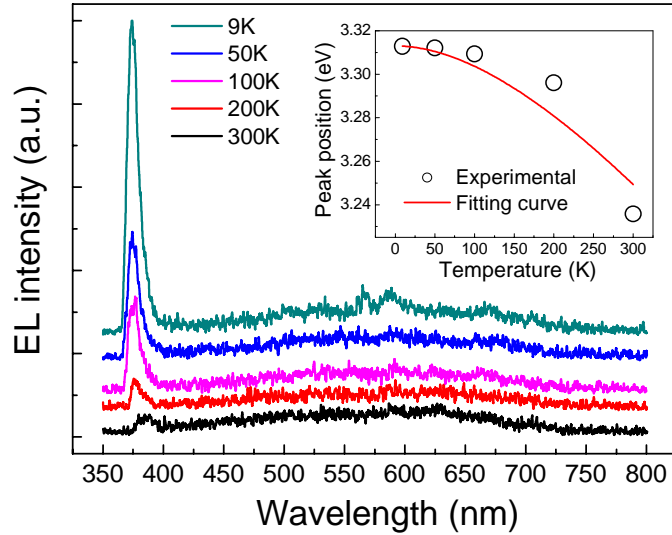


Figure 6 Temperature dependent EL spectra of homojunction diode from 9 K to 300 K under injection current of 30 mA. The spectra are shifted on y-scale for clarity. Inset shows the NBE peak positions as hollow circles against different temperatures, and Varshni fitting is expressed as solid line.

Schirra et al recently assigned the ZnO 3.314 eV emission peak to the transition between free electron and a neutral acceptor level [M. Schirra, R. Schneider, A. Reiser, G. M. Prinz, M. Feneberg, J. Biskupek, U. Kaiser, C. E. Krill, R. Sauer, and K. Thonke, *Physica B*, **401**, 362 (2007)]. However, considering the LT properties of our p-type film [F. X. Xiu, Z. Yang, L. J. Mandalapu, D. T. Zhao, and J. L. Liu, *Appl. Phys. Lett.* **87**, 252102 (2005).], we believe this peak is from band to band exciton recombination. The NBE peak shifts from 373.5 nm to 383.3 nm for temperature ranging from 9 to 300 K, which is shown in the inset of Fig. 6. The temperature dependence of the exciton energy in direct band-gap material follows Varshni equation: $E(T) = E(0) - \alpha T^2 / (T + \beta)$ [T. Shimomura, D. Kim, and M. Nakayama, *J. Lumin.* **112**, 191 (2005)], α and β are fitting parameters which are: $\alpha = 0.00058 eV / K$, and $\beta = 520 K$. These values are close to reported results

from Ref. [T. Shimomura, D. Kim, and M. Nakayama, *J. Lumin.* **112**, 191 (2005) S. J. Chen, Y. C. Liu, J. Y. Zhang, Y. M. Lu, D. Z. Shen, and X. W. Fan, *J. Phys.: Condens. Matter* **15**, 1975 (2003)] for ZnO materials. The peak values agree reasonably with the trend of the fitting curve, which indicates that the red shift of the peak is due to temperature induced band gap variation. In addition to the NBE peak, there seems to be broad radiative deep level emissions ranging from 400 nm to 800 nm. However, the magnitude drop of the deep level emission intensity is much less compared to NBE peak with increasing temperature. This may be attributed to more activation of non-radiative recombinations at higher temperatures, and also the bound exciton emissions quench at higher temperatures by thermal ionization of bound excitons.

Room temperature EL under different injection currents are shown in Fig. 7. For 30 mA injection current, the NBE peak is clearly seen at 383.3 nm (3.24 eV). The deep level emission

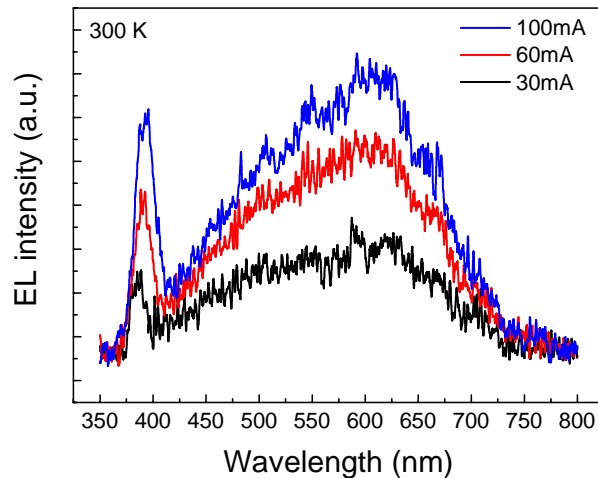


Figure 7 Room temperature EL spectra at different injection current from 30 mA to 100 mA.

at room temperature is mainly centered at 605 nm (2.05 eV), but with a shoulder around 490 nm (2.53 eV). The 490nm band is commonly assigned to intrinsic defects [A. Ortiz, C. Falcony, J. Hernandez, M. Garcia and J. C. Alonso, *Thin Solid Films* **293**, 103 (1997)]. The 605 nm yellow band, is attributed to oxygen interstitials [X. L. Wu, G. G. Siu, C. L. Fu, and H. C. Ong, *Appl. Phys. Lett.* **78**, 2285 (2001).], which is consistent with the fact that the p-type ZnO was prepared in oxygen rich condition. The intensities of both NBE

emission and emissions from deep levels increase with the increase of the injection current. The NBE emission red-shifts from 383.3 nm (30 mA) to 390.9 nm (100 mA). This is also induced by the band gap variations, which result from the increased heating effects during the operation of LEDs. For example, the temperature of the diode is 490 K at the operation current of 100 mA from the inset of Fig.5.

To further investigate the origin of these EL emissions, Photoluminescence (PL) measurements were carried out on a separate piece of the sample annealed at 800 °C for 120 s, a process that was also used during the device fabrication. A 325 nm He-Cd laser was used as the excitation source. The room temperature PL

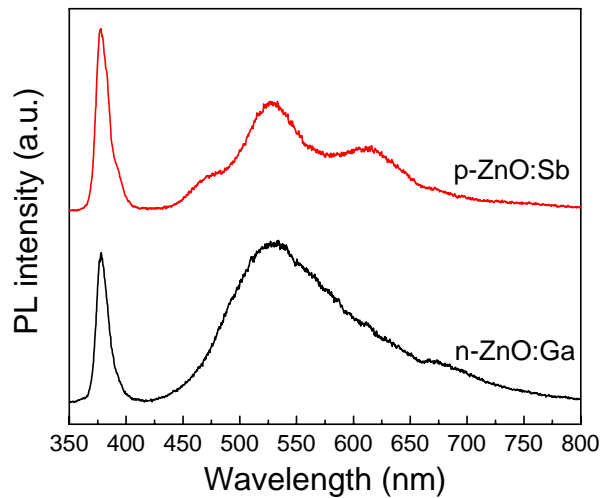


Figure 8 Room temperature PL spectra from Sb-doped p-type ZnO layer and Ga-doped n-type ZnO layer of the homojunction sample.

spectra for both p-type layer and underneath n-type layer are shown in Fig. 8. PL of the n-type ZnO layer was obtained by etching away the p-type ZnO layer. Besides the NBE peak at 377.5 nm, emission bands centered around 520 nm are shown in both spectra and we consider that they are the same peak from n-type ZnO layer since it is commonly attributed to oxygen vacancy [F. K. Shan, G. X. Liu, W. J. Lee and B. C. Shin, *J. Appl. Phys.* **101**, 053106 (2007).]. However, the p-type ZnO layer shows two more peaks at 480 nm and 610 nm which can link with the room temperature EL emissions of 490 nm and 605 nm closely. Thus we believe that radiative recombinations in p-type layer,

including NBE transitions, have contributed mainly to the observed EL spectra. Similar results were also observed in As-doped ZnO diode on GaAs substrate [J. C. Sun, J. Z. Zhao, H. W. Liang, J. M. Bian, L. Z. Hu, H. Q. Zhang, X. P. Liang, W. F. Liu, G. T. Du, *Appl. Phys. Lett.* **90**, 121128 (2007)]. This is reasonable due to the fact that the concentration of holes in p-type ZnO layer is less than the electron concentration of n-type ZnO layer. As a result, the depletion region mostly exists in the p-type layer, and the electron injection from the n-type layer to p-type layer dominates the recombination process.

In conclusion, ZnO homojunction LEDs with the Sb-doped p-type ZnO layer/Ga-doped n-type ZnO layer structure were fabricated and studied. The LEDs with the low resistivity Au/NiO contacts for p-type ZnO showed very good UV emissions at different temperatures and injection currents. This study suggests that Sb-doped p-type ZnO is promising for future ZnO optoelectronics.